4th Conference on Production Systems and Logistics

Laser Drying Of Graphite Anodes For The Production Of Lithium-Ion Batteries – A Process- And Material-Side Analysis For Sustainable Battery Production

Sebastian Wolf[1], Daniel Neb[1], Florian Hölting[2], Barkin Özkan[2], Henning Clever[1], Benjamin Dorn[1], Heiner Hans Heimes[1], Achim Kampker[1]

[1]*Production Engineering of E-Mobility Components (PEM), RWTH Aachen University, Bohr 12, 52072 Aachen, Germany*
[2]*Faculty of Mechanical Engineering, RWTH Aachen University, 52072 Aachen, Germany*

Abstract

In many industries, such as the automotive industry or consumer electronics, the demand for lithium-ion batteries is increasing significantly. The state of the art in battery production is energy-consuming and cost-intensive. The drying process of the viscous active material applied to the conductor foils, together with the coating process, is responsible for more than half of the production costs of an electrode. The high energy consumption of conventional drying processes, such as convection drying, must be reduced. Therefore, lasers are used to dry the active material of the electrodes. Further advantages are the low footprint and the increased process flexibility. Moreover, the controlled energy deposition and the spatially selective heat input increase the energy efficiency of the process innovation laser drying. In this review, the results of experiments on drying anodes by laser are compared with the results of convection drying. For this purpose, different production process parameter combinations and material compositions for anodes are chosen in order to be able to derive the process and material influences on the electrode quality.

Keywords

Battery production; Lithium-ion battery; Electrode manufacturing; Production process innovation; Sustainable production; Laser drying

1. Introduction

In order to achieve the environmental policy climate targets, at both national and international level, the reduction of CO2 emissions in the transport sector is of central importance. These environmental policy climate targets are key factors in the current upheaval in the automotive industry. In recent years, automotive manufacturers have increasingly shifted their focus away from combustion engines to electromobility [1].

However, this upheaval is associated with many challenges. Two major challenges are the high cost of electric vehicles (EV) and the reduction of the carbon footprint over the total life cycle. The production costs of EVs are significantly higher due to the battery as a key component compared to conventional drives. [2, 3] One of the main influencing factors for the costs and energy consumption of battery production is the drying process with its high investing costs, high energy consumption of natural gas and resulting operating costs. [4, 5, 6] Küpper et al. showed that the coating and drying process is responsible for 54 % of the electrode production costs while these constitute about 39 % of the costs of battery cell production. Therefore, the coating and drying process makes up about 21 % of the total battery cell production costs [7].

DOI: https://doi.org/10.15488/13455
ISSN: 2701-6277

In recent years, research began on laser drying as a potential substitute for the conventional drying process. Lasers have already been used in industry in many areas as part of a variety of processes such as laser cutting, laser welding, laser processes for surface treatment or drilling and ablation with lasers [8]. Vedder et al. already showed that the drying of water-based anodes or cathodes containing lithium iron phosphate as active material is basically possible with almost similar quality regarding the conventional drying process [9]. The key advantages of drying electrodes by laser instead of convection drying are their high energy efficiency and small machine footprint which potentially results in lower invest and operating costs.

Nevertheless, the factors influencing the electrode quality dried by laser have hardly been researched. This publication aims to continue research in the field of laser drying of electrodes. The material and process sided factors influencing the drying quality of electrodes will be discussed. In the context of this publication, the electrodes have undergone the processes of mixing, coating, and either convection or laser drying.

2. Experimental Set-up

The battery production process is divided into three sections: Electrode manufacturing, cell assembly and cell finishing. In order to classify the subsequent experimental set-up, the process chain, showed in figure 1, of electrode production is described in detail and discussed below regarding laser drying [10].

Figure 1: Electrode manufacturing process chain

2.1 Processes in electrode manufacturing

The first manufacturing step is mixing. Here, binders such as styrene-butadiene rubber (SBR), carboxymethyl cellulose (CMC) and solvent are added to the active material (graphite). Furthermore, added conductive carbon black increases the electrical conductivity of the final cell [11]. The individual components are precisely weighed and stirred in a mixing unit. In addition to the material composition, process parameters like speed and mixing time determine the mixing process [4].

The mixing process is followed by the coating and drying of the slurry on the carrier film in a roll-to-roll process. A pump conveys the slurry evenly to the coating tool, which depends on the application method used. A distinction is made here between slot die, doctor blade or coating roller processes. [12] The carrier film is unwound from a coil at a defined web speed. The coating thickness can be varied depending on the web speed and the set pump speed with which the slurry is transported to the coating tool. In the case of the slot die application tool, the choice of shim plate and the distance between slot die and foil influence the gap width and thus the coating width and thickness. [4]

The structure and properties of the electrodes are also influenced by the subsequent drying process. The drying process has a significant influence on the quality of the cells and the production scrap rates. The task of drying is to dissolve the solvents from the applied coating and thus to dry the coating. Convection drying is the most common variant in practice, as the air flow generated is also used to remove the evaporated solvents [13]. Other drying options include infrared and laser dryers. This is followed by calendering, in which the electrode foil undergoes a rolling process. Then the coated film goes through the process steps of slitting and vacuum drying. After that, the cell is assembled, before the quality properties are finally checked for the last time in the cell finalization. [4]

2.2 Trial setup und process parameters

For the coating process in the underlying experimental setup, a one-sided coating system with a slot die is used. The web speed is adjusted by a drive located on the unwinder mandrel. In this way, different process speeds can be achieved. The slurry is conveyed to the slot die by a gear pump. The flow rate can be regulated by varying the pump speed.

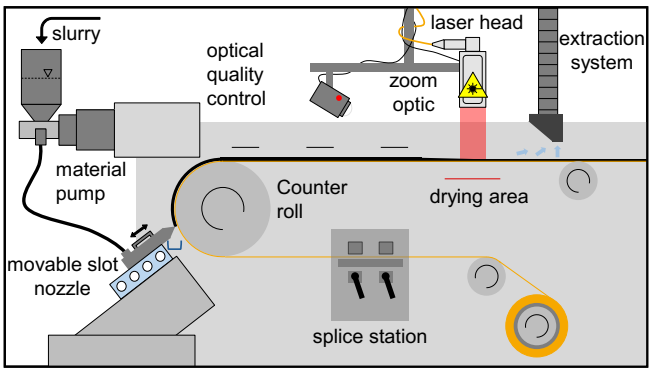

Figure 2: construction of the coating and drying process

After the coating process, the active material is dried on the 10 µm thick copper substrate foil. Two independent options are available for this in the experimental set-up used. In the first step, drying is done by a convection oven with a length of 3.5 m. Therefore, two drying chambers are present in which the solvent is evaporated by hot air. The temperatures in the two chambers can be set manually and differ. The second drying option shown in figure 2 is a diode laser. The laser used has a maximum output power of 8,000 W. In addition, a wavelength range of 900 to 1,080 nm is available. The zoom optics of the laser in the roll-to-roll process are located behind the slot die. The radiation hits the carrier foil perpendicularly on a 16 x 17 cm laser spot. A control module allows the laser power and thus intensity to be adjusted. After the drying process, the dried film is wound onto a coil with the help of a web edge control system.

Four different compositions, shown in Table, are mixed. Mixture 1 is a typical slurry recipe that is used in the industry in terms of substance concentration and used materials [14]. The other recipes are characterized by increasing the proportion of SBR (mixture 2), CMC (mixture 3) or solvent (mixture 4).

Table 1: Material composition of four tested mixtures

Mixture	1	2	3	4
Components of the mixture	Mass percentage [wt%]	Mass percentage [wt%]	Mass percentage [wt%]	Mass percentage [wt%]
Graphite	42.3	42	42.2	41.5
SBR	3.4	4.2	3.4	3.3
CMC	0.9	0.9	1.1	0.9
Conductive carbon black	0.4	0.4	0.4	0.4
Solvent	53	52.5	52.9	53.9

In addition, the process parameters of the coating and drying tests are varied. A distinction is made between the web speed, the pump speed and the heating temperatures of the two chambers or the laser intensity, whereby either convection or laser drying is used. Table 2 shows the used parameter sets of the coating process.

Table 2: Process parameter sets

Process parameter sets	1	2	3	4	5	6
Web speed [m/min]	0.8	0.8	1.3	1.3	1.8	1.8
Flow rate [cm³/min]	21	25.2	30.8	33.6	44.8	47.6
Temperature of heating chamber 1 [°C]	130	130	130	130	130	130
Temperature of heating chamber 2 [°C]	110	110	110	110	110	110
Laser intensity [W/cm²]	2.33	2.33	2.68	2.68	3.22	3.22
Total energy input per area [J/cm²]	29.71	29.71	21.03	21.03	18.25	18.25
Wet film thickness [µm]	169	203	153	167	161	171

The aim of the different compositions and process parameters is to investigate the influence on residual moisture content and the adhesion of the active material to the copper foil as the key quality parameters of the electrode drying process.

3. Process-sided evaluation

For the evaluation on the process side, the conducted analysis concentrates on the first and the fourth material compositions from Table 1 (mixture 1 and 4). A higher solvent content results in a more homogeneous mixture compared to the standard mixture. To assess the quality of the electrodes, samples of the coated foil are examined with regard to residual moisture and adhesion. The residual moisture is determined using a residual moisture meter and is measured by drying the sample and measuring the change in weight in parallel. The residual moisture content thus results from the difference in weight of the sample between the time before and after the drying process. To measure the tensile force, a punched-out sample of the coated film is stuck onto a stamp with adhesive tape. Another stamp (again equipped with adhesive tape) then moves onto the sample and presses it onto the other stamp with a previously set force. After that, the stamp is moved upwards at a constant speed. The force at which the coating is released from the carrier film is measured.

3.1 Convection drying

In order to obtain reference values for the assessment of laser drying, convection drying is discussed first. Figure 3 shows the results of the residual moisture and adhesion tests over the six sets of process parameters investigated with convection drying, which can be found in Table 2. The temperatures in the chambers of the dryer were kept constant throughout the drying process.

The residual moisture results of the mixture 4 are clearly above those of the mixture 1. This can be explained by the almost 1 % higher mass fraction of the solvent, which does not evaporate equally to the standard mixture during drying. In addition, the residual moisture increases when the flow rate ceteris paribus (c.p.) is increased. This can be seen in the transitions from parameter set 1 to 2, 3 to 4 and 5 to 6. An increased flow rate results in a higher wet film thickness, which means that more coating has to be dried in the same

time. This results in a higher residual moisture content. Therefore, it can be seen that an increased wet film thickness results in an increase in residual moisture.

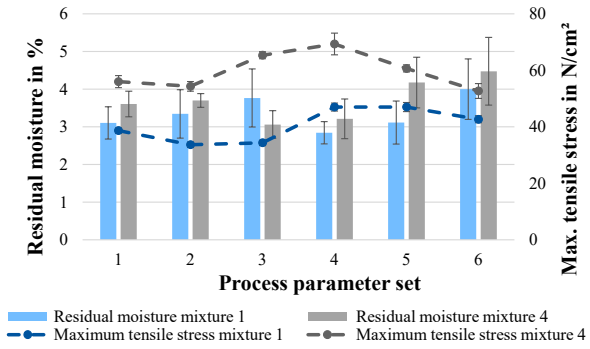

Figure 3: Residual moisture and maximum tensile stress of convection dried anodes

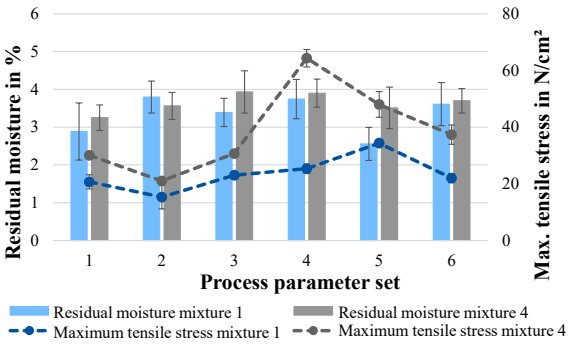

Figure 4: Residual moisture and maximum tensile stress of laser dried anodes

The analysis of the adhesion results shows a higher tensile stress of the mixture with increased solvent content compared to the standard mixture across all process parameter sets. This can be explained by an improved homogeneity of the slurry. The binder CMC has a high water absorption and can develop its potential better with an increased solvent content. This effect is explained in chapter 4.

At web speeds of 0.8 and 1.8 m/min, an increase in flow rate c.p. results in a decrease in tensile stress. A higher wet film thickness results in a lower tensile stress of the coating to the carrier film. This was not confirmed at a web speed of 1.3 m/min, an anomaly was revealed here. However, the standard mixture at process parameter set 3 also has a higher residual moisture than the mixture 4. This suggests that these samples should not be given the same importance as the other web speeds. The highest tensile stress of 69.33 N/cm² results from the solvent mixture with a web speed of 1.3 m/min and a flow rate of 33.6 cm³/min. The residual moisture is also low (3.21 %) across the process parameter sets at this web speed and the lower flow rate. Only the standard compound at a web speed of 1.3 m/min and a flow rate of 33.6 cm³/min shows a lower residual moisture. However, this results in a significantly lower tensile stress, which clearly shows that the solvent mixture is superior to the standard mixture in convection drying in terms of residual moisture and adhesion.

3.2 Laser drying

The diode laser is used to dry the electrodes. The laser spot on the electrode surface is 16 cm wide (corresponds to the coating width on the film) and 17 cm long (in the direction of movement of the film). First, a laser intensity was defined experimentally for each web speed at which the coating is dry, but the surface condition is not impaired by an excessive intensity. This results in a laser intensity of 2.33 W/cm² (total energy input per area of 29.71 J/cm²) for parameter sets 1 and 2, an intensity of 2.68 W/cm² (total energy input per area of 21.03 J/cm²) for parameter sets 3 and 4 and an intensity of 3.22 W/cm² (total energy input per area of 18.25 J/cm²) for parameter sets 5 and 6. It is noticeable here that the correlation between the increase in web speed and the increase in laser intensity is not linear in the lower tenth of the possible laser power.

In order to achieve sufficient drying results, the laser intensity does not have to be nearly doubled when the web speed increases from 0.8 m/min to 1.8 m/min (corresponds to an increase of 225 % and raise in laser intensity of 20 %). The diode laser achieves more precise focusing for higher intensities (above 10 % of the maximum capacity), so that for the low web speeds of 0.8 m/min and 1.3 m/min a higher total energy input per area is required to achieve a sufficient drying result.

3.2.1 Adhesion

Figure 4 shows the maximum tensile stress of mixture 1 and mixture 4 anodes. Here, three samples per process parameter combination were evaluated and the mean value of these three were determined. The standard deviation is shown by means of a corridor around the points.

The tensile stress of mixture 4 is higher than that of mixture 1 for all process parameter sets. This is due to the improved homogeneity of the slurry. For the web speeds of 0.8 and 1.8 m/min, increasing the flow rate c.p. results in a low tensile stress (parameter set 1 to 2 and 5 to 6). At the web speed of 1.3 m/min, the tensile stress increases when the flow rate c.p. is raised, and even significantly for mixture 4. To figure out the reason for this, Table 2 shows the wet film thicknesses of the process parameter combinations. From parameter set 1 to parameter set 2 the flow rate increases by 20 %, from 3 to 4 by 9 % and from parameter set 5 to 6 by 6 %. These percentage changes are also reflected in the wet film thicknesses. A too high wet film thickness has a negative effect on the distribution of the binders, which reduces the adhesion of the coating. Process parameter set 3 has a lower wet film thickness compared to parameter set 1, but also a lower total energy input per area, resulting in similar tensile stress results to parameter set 1. When the flow rate is increased to 33.6 cm^3/min the wet film thickness increases to 167 µm. With mixture 4 the tensile stress doubles, with the mixture 1 there is also an increase in tensile stress. This can be attributed to the fact that the laser radiation at parameter set 3 has influenced the effect of the binders due to the lower wet film thickness. The binders cannot exert their property of supporting adhesion. This is probably due to the binders were partially destroyed by the laser intensity. This effect can be compensated with an increased wet film thickness, as the laser has to dry more coating in the same time. The positive adhesion property of the binders thus remains, which is shown by the increase in tensile stress. An increase in the wet film thickness (process parameter set 6) leads to a decrease in the tensile stress, as with the web speed of 0.8 m/min. Finally, it can be stated that a too low wet film thickness has negative effects on the binders (parameter set 3). Increasing the wet film thickness can avoid this effect. However, there is a limit here. If the wet film thicknesses are above 170 µm, this results in a drop in the tensile stress. For mixture 1, a combination of a web speed of 1.8 m/min with a flow rate of 44.8 cm^3/min and a total energy input of 18.25 J/cm^2 is optimal, whereas for mixture 4, a web speed of 1.3 m/min with a flow rate of 33.6 cm^3/min and a total energy input of 21.03 J/cm^2 provides the highest stresses.

3.2.2 Residual moisture

The residual moisture values of mixture 1 and mixture 4 are listed in Figure 4. The results of the residual moisture test for all parameter sets (except parameter set 2) are higher for mixture 4 than for mixture 1. This can be explained by the increased solvent content, which cannot evaporate in the same time. When enlarging the flow rate c.p. (parameter set 1 to 2, 3 to 4 and 5 to 6) the residual moisture increases. The increased flow rate results in a higher wet film thickness, which means that more solvent has to be dried and the residual moisture increases. Only with the solvent mixture at a web speed of 1.3 m/min (parameter set 3 and 4), the residual moisture remains constant. If the standard deviations of the values are considered, this irregularity can be eliminated. The residual moisture values are in a similar range over all web speeds because the intensity has been adjusted so that the coating is visible dry. For the first process parameter set, the residual moisture is just under 3 %. If the flow rate is increased by 20 % (parameter set 2), the residual moisture increases by more than 30 % for mixture 1. With mixture 4, on the other hand, only a 10 % increase in residual moisture from parameter set 1 to parameter set 2 is discernible. From this it can be deduced that there is no direct linear relationship between flow rate and residual moisture. Furthermore, an interplay between residual moisture and adhesion can be observed. At the web speeds of 0.8 m/min and 1.8 m/min it is evident that a higher residual moisture leads to a lower adhesion (parameter sets 2 and 4). This can possibly

be explained by a better utilisation of the adhesion properties of the binders at a lower moisture content of the coating [15].

In addition, process parameter set 5 provides better quality parameters for both mixture 1 and mixture 4 compared to the other five parameter sets. For mixture 1, parameter set 5 has the lowest residual moisture of the series of 2.56 % and for mixture 4 the second lowest residual moisture of 3.51 %. The total energy input per area of 18.25 J/cm² is sufficient for a dry coating result. The tensile stresses for this process parameter set are also in the upper range of the measurement series. Therefore, a suitable process window can be characterised with this process combination.

Moreover, the results of the residual moisture of the laser drying are compared with those of the convection drying. Overall, both mixture 1 and mixture 4 showed slightly better results than the residual moisture of convection drying on average for the first six sets of process parameters. The average value for the mixture 1 was approximately 0.03 % lower for laser drying than for convection drying. For mixture 4 there was a difference of approximately 0.07 %. Firstly, the results of mixture 1 are considered in detail. For process parameter set 1, the residual moisture by laser drying is below that of convection drying. If the flow rate is increased (parameter set 2), a higher laser intensity is needed to reach the residual moisture content of convection drying. The same findings can be transferred for the web speed of 1.3 m/min (parameter sets 3 and 4). At the high web speeds of 1.8 m/min, the residual moisture results of laser drying with both flow rates tested are below those of convection drying. Even with a reduced energy input per area of 15.19 J/cm² (parameter set 8), a comparable residual moisture to convection drying can be achieved. This is 0.09 % higher than that of convection drying (parameter set 5). This negligible difference can be accepted due to a significantly higher tensile stress. Besides, the residual moisture results of mixture 4 of laser drying and convection drying are compared in detail. For a web speed of 0.8 m/min, the residual moisture values of laser drying for both flow rates are below those of convection drying (parameter sets 1 and 2).

At a web speed of 1.3 m/min, the residual moisture values of convection drying cannot be achieved with the selected laser intensity of 21.03 J/cm². The reason for this is the increased solvent content. At the high web speeds of 1.8 m/min, laser drying with the selected energy input per area of 18.25 J/cm² dominates convection drying at both flow rates tested.

4. Material-side evaluation

4.1 Material-sided influences

Beside the concentration of solvent, the concentration of CMC is one of the main material-sided influencing factors on the residual moisture. As a result of the high water reactivity of CMC, there is increased water absorption [16]. This leads to a higher residual moisture content of the coating after drying. The tensile stresses after drying are positively influenced mainly by higher binder concentration, lower solvent concentration and film thickness and a higher homogeneity. [15, 17, 18]. Furthermore, the understanding of the binders CMC and SBR is important. While CMC is used as a thickening and setting agent, SBR increases the elasticity of the coating [19, 20]. Consequently, the shrinkage forces acting on the coating during drying can be absorbed favorably. If the SBR concentration is too low, cracks may occur because of the plastic absorption of these shrinkage forces [21]. Furthermore, these cracks can lead to adhesion losses [22]. Regarding the surface finish, a higher binder concentration also has a positive effect on the surface quality as a result of better filling of the cavities, especially for SBR. [6, 23]

4.2 Residual moisture

The reductions of the residual moisture contents, which were achieved by laser drying in comparison to convection drying, are shown in Figure 5. Here, the standard deviations are not to be understood as drying or measuring accuracy, but rather the range in which the measured values of the parameters sets 1, 3 and 5 lie.

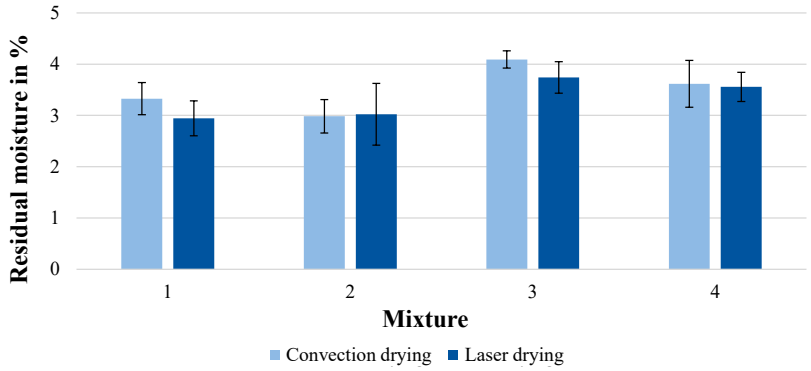

Figure 5: Residual moisture of all mixtures dried by

First, the residual moisture contents after convection drying are considered. The humidity after convection drying of mixture 2 has the lowest average measured value because of the lowest concentration of solvent. Further on, mixture 3 has the highest average residual moisture. This can be attributed to a higher water absorption due to increased CMC (see section 4.1). Mixture 1 shows the second lowest average measured humidity after convection drying. It is higher compared to mixture 2 due to an increased concentration of solvent. Apart from that, mixture 4 exhibits a higher average residual moisture than mixture 1 also as a result of the increased concentration of solvent and has a lower residual moisture than mixture 3. This is potentially due to the effect of water absorption on the humidity after drying, caused by the increased proportion of CMC, is stronger than the effect of the higher concentration of solvent regarding the mixture with a higher proportion of solvent.

In order to analyze the results after laser drying, the absorption coefficient of the coating in particular must be considered, because the absorption of laser radiation is determined by the absorption coefficient. It is essentially influenced by the graphite concentration of a material composition. [24] In Table 3, the graphite concentrations and the differences between the residual moistures of the coatings after laser drying and convection drying are shown. The results of the convection drying are used as the reference values. It is clearly seen that the highest reductions of the residual moisture contents were reached by the mixtures with the highest mass percentage of graphite, the standard mixture (total graphite concentration of 42.3 %) and the mixture with an increased proportion of CMC (total graphite concentration of 42.2 %). The mixture with an increased proportion of solvent shows a reduction of residual moisture after laser drying of 1.67 % in comparison to the residual moisture after convection drying.

Table 3: Graphite concentrations and differences of laser-dried and conventionally dried mixtures

	Standard mixture	CMC mixture	SBR mixture	Solvent mixture
Graphite concentration	42.3	42.2	42.0	41.5
Difference of residual moisture	-11.71 %	-8.56 %	+1.34 %	-1.67%

Mixture 2 shows about 1.34 % higher residual moisture after laser drying in comparison to convection drying. Regarding the graphite contents, it is unexpected that a higher reduction of the average measured

humidity was achieved after laser-based drying of mixture 4 than after laser-based drying of mixture 2. Looking at the results of the residual moisture testing of each parameter, mixture 2 shows an unexpectedly high residual moisture content after laser-based drying by parameter set 2. This unexpectedly high value caused a higher average measured humidity after laser-based drying of this mixture.

To sum up the results of the residual moisture tests, it is shown that the higher concentrations of solvent and CMC lead to higher moisture contents after the drying process. Furthermore, regarding the laser-based drying the graphite concentration significantly influences the humidity due to higher absorption coefficients. Therefore, higher concentrations of graphite lead to higher absorption coefficients and these in turn lead to lower residual moisture contents.

4.3 Adhesion

The conventionally dried mixture 3 shows the highest average maximum tensile stresses due to higher binder concentration (see section 4.1). The conventionally dried mixture 4 has the second highest average maximum tensile stresses due to higher homogeneity despite an increased proportion of solvent (see section 4.1).

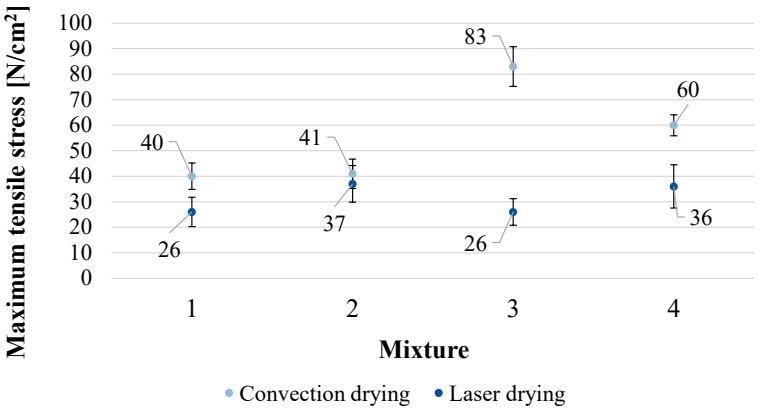

Figure 6: Maximum adhesion forces of all mixtures dried by

Furthermore, the conventionally dried mixture 1 and mixture 2 have the lowest average maximum tensile stresses. Therefore, the conventionally dried standard mixture has no significant losses regarding its adhesion. Potentially, the shrinking forces occurring during convection drying at the temperatures of 110 °C and 130 °C are comparatively low. As a result, the SBR had no significant effect regarding its improvement of elastically force absorption due to low shrinking forces. In Figure 6 the maximum tensile stresses are shown for the convection drying and laser-based drying. Here, the standard deviations are not to be understood as drying or measuring accuracy, but rather the range in which the measured values of the parameters sets 1, 3 and 5 lie. For every mixture, the maximum tensile stresses after laser-based drying are lower in comparison to convection drying. Especially the laser-dried mixture 3 shows the highest loss of tensile stresses in comparison to convective drying. Looking at the relative losses of tensile stresses after laser-based drying, the high laser intensity potentially damages the CMC. This explains the massive tensile stress losses of the laser-based drying of the mixture with an increased proportion of CMC. The loss of 40 % of tensile stresses of the laser-dried mixture 4 is higher than the loss of 35 % of tensile stresses of the laser-dried mixture 1. This potentially leads back to the relatively higher proportion of SBR in mixture 1 (3.4 %) than in mixture 4 (3.3 %). SBR can potentially cause a better absorption of the shrinking forces that occur during laser drying.

5. Conclusion

In summary, it could be shown that comparable residual moisture results and slightly lower to equivalent adhesion forces of the active material on the carrier film can be achieved with laser drying compared to convection drying. In particular, the graphite concentration has a significant influence on the residual moisture of the active material due to the high degree of absorption in the wave spectrum of the diode laser used. Furthermore, it could be shown that the solvent concentration and the amount of binders used, such as CMC and SBR, have an influence on the drying result. Regarding adhesion forces, it was shown that CMC is more sensitive to binder degradation at high laser intensities compared to SBR. This can lead to significantly high losses in the maximum tensile stresses for adhesion to the carrier film. Thus, lower laser intensities should be used to reduce the adhesion loss compared to convection drying. SBR seems to be a suitable binder for laser drying, as the shrinkage forces affecting the film and the coating during the drying process can be absorbed more elastically. For the process side evaluation, it can be stated that due to the non-linear power curve of the laser in the lower tenth of the retrievable power, there are challenges in correctly setting the laser intensity and the intensity cannot be easily scaled. Increasing the flow rate c.p. increases the wet film thickness and thus also the residual moisture. In addition, the tensile stress decreases with increasing residual moisture, as the binders can no longer fully exploit their adhesive properties at high moisture levels.

In conclusion, electrode drying by laser proves to be a promising alternative due to the low energy and space requirements. In the future, it should be investigated how laser drying can be scaled up to higher web speeds, for example by connecting several laser modules in series. Furthermore, it is necessary to compare the experimental results of other laser drying processes (e.g. VCSEL) with the experimental results of this paper. Another advantage of laser drying compared to convection drying is the faster controllability of the system, as the energy used can be adjusted without delay and long warm-up phases of the oven are avoided. Further research is needed to investigate the interdependencies of the laser drying process on the final cell quality and to further detail a process window for laser drying of anodes and cathodes for optimal electrode quality.

Acknowledgements

This work is part of the Project IDEEL. The project has received funding from the German Federal Ministry of Education and Research (BMBF) under the funding code 03XP0414D. The authors are responsible for the content of this publication.

References

[1] Attias, D., 2016. The Automobile Revolution. Towards a New Electro-Mobility Paradigm. Cham: Springer International Publishing.

[2] Kampker, A., Vallée, D., Schnettler, A., 2018. Elektromobilität. Berlin, Heidelberg: Springer Berlin Heidelberg.

[3] Helms, H., Kämper, C., Biemann, K., Lambrecht, U., Jöhrens, J., Meyer, K., 2019. Klimabilanz von Elektroautos. Einflussfaktoren und Verbesserungspotenzial. Agora Verkehrswende.

[4] Heimes, H., Kampker, A., Lienemann, C., Offermanns, C., Locke, M., 2018. Produktionsprozess einer Lithium-Ionen-Batteriezelle.

[5] Liu, Y., Zhang, R., Wang, J., Wang, Y., 2021. Current and future lithium-ion battery manufacturing. In: iScience 24 (4), S. 102-332.

[6] Wood, D. L., Quass, J. D., Li, J., Ahmed, S., Ventola, D., Daniel, C., 2018. Technical and economic analysis of solvent-based lithium-ion electrode drying with water and NMP. In: Drying Technology 36 (2), S. 234–244.

[7] Küpper, D., Kuhlmann, K., Wolf, S., Pieper, C., Xu, G., Ahmad, J., 2018. The Future of Battery Production for Electric Vehicles. Hg. v. The Boston Consulting Group.

[8] Bogue, R., 2015. Lasers in manufacturing: a review of technologies and applications. In: Assembly Automation 35 (2), S. 161–165.

[9] Vedder, C., Hawelka, D., Wolter, M., Leiva, D., Stollenwerk, J., Wissenbach, K., 2016. Laser-based drying of battery electrode layers. In: International Congress on Applications of Lasers & Electro-Optics. ICALEO® 2016: 35th International Congress on Applications of Lasers & Electro-Optics. San Diego, California, USA, October 16–20, 2016: Laser Institute of America, N501.

[10] Neb, D., Kim, S., Clever, H., Dorn, B., Kampker, A., 2022. Current advances on laser drying of electrodes for lithium-ion battery cells

[11] Wöhrle, T., 2013. Lithium-Ionen-Zelle. In: Reiner Korthauer (Hg.): Handbuch Lithium-Ionen-Batterien. Berlin, Heidelberg: Springer Berlin Heidelberg, S. 107–117.

[12] Kampker, A., Hohenthanner, C., Deutskens, C., Heimes, H., Sesterheim, C., 2013. Fertigungsverfahren von Lithium-Ionen-Zellen und -Batterien. In: Reiner Korthauer (Hg.): Handbuch Lithium-Ionen-Batterien. Berlin, Heidelberg: Springer Berlin Heidelberg, S. 237–247.

[13] Röth, T., Kampker, A., Deutskens, C., Kreisköther, K., Heimes, H., Schittny, B., 2018. Entwicklung von elektrofahrzeugspezifischen Systemen. In: Achim Kampker, Dirk Vallée und Armin Schnettler (Hg.): Elektromobilität. Berlin, Heidelberg: Springer Berlin Heidelberg, S. 279–386.

[14] Liu, D., Chen, L., Liu, T., Fan, T., Tsou, E., Tiu, C., 2014. An Effective Mixing for Lithium Ion Battery Slurries. In: ACES 04 (04), S. 515–528.

[15] Jaiser, S., Sanchez Salach, N., Baunach, M., Scharfer, P., Schabel, W., 2017. Impact of drying conditions and wet film properties on adhesion and film solidification of lithium-ion battery anodes. In: Drying Technology 35 (15), S. 1807–1817.

[16] Eser, J. C., Wirsching, T., Weidler, P.G., Altvater, A., Börnhorst, T., Kumberg, J., 2020. Moisture Adsorption Behavior in Anodes for Li‐Ion Batteries. In: Energy Technol. 8 (2), S. 1801162.

[17] Vuorilehto, K., 2013. Materialien und Funktion. In: Reiner Korthauer (Hg.): Handbuch Lithium-Ionen-Batterien. Berlin, Heidelberg: Springer Berlin Heidelberg.

[18] Haselrieder, W., Westphal, B., Bockholt, H., Diener, A., Höft, S., Kwade, A., 2015. Measuring the coating adhesion strength of electrodes for lithium-ion batteries. In: International Journal of Adhesion and Adhesives 60, S. 1–8.

[19] Yen, J., Chang, C., Lin, Y., Shen, S., Hong, J., 2013. Effects of Styrene-Butadiene Rubber/Carboxymethylcellulose (SBR/CMC) and Polyvinylidene Difluoride (PVDF) Binders on Low Temperature Lithium Ion Batteries. In: Journal of The Electrochemical Society, S. 1812.

[20] Liu, W.-R., Yang, M.-H., Wu, H.-C., Chiao, S. M., Wu, N.-L., 2005. Enhanced Cycle Life of Si Anode for Li-Ion Batteries by Using Modified Elastomeric Binder. In: Electrochemical and Solid-State Letters, S. 102-103.

[21] Fischer, S. B., Koos, E., 2021. Using an added liquid to suppress drying defects in hard particle coatings. In: Journal of colloid and interface science, S. 1231.

[22] Ramier, J., Da Costa, N., Plummer, C.J.G., Leterrier, Y., Månson, J.-A.E., Eckert, R., Gaudiana, R. 2008. Cohesion and adhesion of nanoporous TiO2 coatings on titanium wires for photovoltaic applications. In Thin Solid Films, S. 1908.

[23] Park, J., Ahn, K., 2021. Controlling Drying Stress and Mechanical Properties of Battery Electrodes Using a Capillary Force-Induced Suspension System. In: Ind. Eng. Chem. Res. 60 (13), S. 4873–4882.

[24] Pawlowski, L. (1999): Thick Laser Coatings: A Review. In: Journal of Thermal Spray Technology, S. 281.

Biography

Sebastian Wolf (*1997) is research associate in the group Battery Production Management at the Chair of Production Engineering of E-Mobility Components (PEM) at RWTH Aachen University, where he also studied Mechanical Engineering and Business Administration.

Daniel Neb (*1992) is research associate in the group Battery Production Management at PEM of RWTH Aachen University, where he also studied Mechanical Engineering with a specialization in Automotive Technology.

Florian Hölting (*1997) has been student assistant at PEM of RWTH Aachen University since 2021, where he also studied Mechanical Engineering and Business Administration.

Barkin Cem Özkan (*1998) studied Mechanical Engineering and Business Administration with a specialization in production technology and Operations Research and Management at RWTH Aachen University.

Henning Clever (*1992) is research associate at PEM of RWTH Aachen University since 2019 and group lead for the research group Battery Production Management since 2021. He studied Mechanical Engineering specializing in Production Engineering at RWTH Aachen University.

Benjamin Dorn (*1990) is chief engineer for Production Technology and Organization at PEM of RWTH Aachen University. He studied Mechanical Engineering and Business Administration there.

Heiner Hans Heimes (*1983) was chief engineer of the newly established Chair of PEM of RWTH Aachen University from 2015 to 2019. Since 2019, Dr.-Ing. Heimes has held the role of executive chief engineer at PEM.

Achim Kampker (*1976) is head of PEM at RWTH Aachen. He also acts as member of the executive board of the Fraunhofer FFB in Münster. Achim Kampker is involved in various expert groups of the federal and state governments.